



## Article

# Assessing Forest Species Diversity in Ghana's Tropical Forest Using PlanetScope Data

Elisha Njomaba <sup>1,\*</sup> , James Nana Ofori <sup>2</sup> , Reginald Tang Guuroh <sup>2,3</sup>, Ben Emunah Aikins <sup>4</sup>,  
Raymond Kwame Nagbija <sup>5</sup> and Peter Surovy <sup>1</sup>

<sup>1</sup> Faculty of Forestry and Wood Sciences, Czech University of Life Sciences Prague, Kamycka 129, 165 00 Prague, Czech Republic; surovy@fld.czu.cz

<sup>2</sup> Biodiversity Research/Systematic Botany, University of Potsdam, Maulbeerallee 1, 14469 Potsdam, Germany; james.nana.ofori@uni-potsdam.de (J.N.O.); rtguuroh@csir-forig.org.gh (R.T.G.)

<sup>3</sup> CSIR-Forestry Research Institute of Ghana, Kumasi P.O. Box UP 63, Ghana

<sup>4</sup> School of Public Health, College of Health Sciences, University of Ghana, Accra P.O. Box LG 13, Ghana; benaikins56@gmail.com

<sup>5</sup> Faculty of Geoinformation Science & Earth Observation, Department of Natural Resource Management, University of Twente, Drienerlolaan 5, 7522 NB Enschede, The Netherlands; r.k.nagbija@student.utwente.nl

\* Correspondence: njomaba@fld.czu.cz; Tel.: +420-773-101-545

**Abstract:** This study utilized a remotely sensed dataset with a high spatial resolution of 3 m to predict species diversity in the Bobiri Forest Reserve (BFR), a moist semi-deciduous tropical forest in Ghana. We conducted a field campaign of tree species measurements to achieve this objective for species diversity estimation. Thirty-five field plots of 50 m × 20 m were established, and the most dominant tree species within the forest were identified. Other measurements, such as diameter at breast height (DBH ≥ 5 cm), tree height, and each plot's GPS coordinates, were recorded. The following species diversity indices were estimated from the field measurements: Shannon–Wiener ( $H'$ ), Simpson diversity index ( $D_2$ ), species richness ( $S$ ), and species evenness ( $J'$ ). The PlanetScope surface reflectance data at 3 m spatial resolution was acquired and preprocessed for species diversity prediction. The spectral/pixel information of all bands, except the coastal band, was extracted for further processing. Vegetation indices (VIs) (NDVI—normalized difference vegetation index, EVI—enhanced vegetation index, SRI—simple ratio index, SAVI—soil adjusted vegetation index, and NDRE—normalized difference red edge index) were also calculated from the spectral bands and their pixel value extracted. A correlation analysis was then performed between the spectral bands and VIs with the species diversity index. The results showed that spectral bands 6 (red) and 2 (blue) significantly correlated with the two main species diversity indices ( $S$  and  $H'$ ) due to their influence on vegetation properties, such as canopy biomass and leaf chlorophyll content. Furthermore, we conducted a stepwise regression analysis to investigate the most important spectral bands to consider when estimating species diversity from the PlanetScope satellite data. Like the correlation results, bands 6 (red) and 2 (blue) were the most important bands to be considered for predicting species diversity. The model equations from the stepwise regression were used to predict tree species diversity. Overall, the study's findings emphasize the relevance of remotely sensed data in assessing the ecological condition of protected areas, a tool for decision-making in biodiversity conservation.

**Keywords:** PlanetScope data; Shannon diversity; species richness; tropical forest; species diversity indices; spectral bands; vegetation indices; ecosystem services; biodiversity conservation; spatial resolution



**Citation:** Njomaba, E.; Ofori, J.N.; Guuroh, R.T.; Aikins, B.E.; Nagbija, R.K.; Surovy, P. Assessing Forest Species Diversity in Ghana's Tropical Forest Using PlanetScope Data. *Remote Sens.* **2024**, *16*, 463. <https://doi.org/10.3390/rs16030463>

Academic Editor: Michael Sprintsin

Received: 28 November 2023

Revised: 17 January 2024

Accepted: 23 January 2024

Published: 25 January 2024



**Copyright:** © 2024 by the authors. Licensee MDPI, Basel, Switzerland. This article is an open access article distributed under the terms and conditions of the Creative Commons Attribution (CC BY) license (<https://creativecommons.org/licenses/by/4.0/>).

## 1. Introduction

Forest biodiversity is essential to terrestrial ecosystems and provides humanity with many crucial ecosystem goods and services [1]. Some vital ecosystem services include the forest nutrient cycle, headwater conservation, and carbon storage [2]. Factors including

climate change, soil erosion, species introduction, and invasion cause changes in forest diversity [3]. Therefore, properly managing forest resources can help conserve biodiversity, water, and soil within forest ecosystems [4].

Tropical forests have a unique reputation for their global role in biodiversity conservation, climate stability, and human well-being [5]. Tropical forests also host the largest biodiversity in terrestrial ecosystems and play a fundamental role in the carbon cycle. Therefore, improvements in forest monitoring, such as understanding species richness and ecological and structural traits [6], are relevant for implementing climate change-related agreements for biodiversity conservation [7]. Long-term biodiversity conservation depends on knowledge of the vegetation structure, species richness, diversity, and ecological characteristics.

Measuring species diversity includes two components: richness and evenness. Richness refers to the total number of species within a given area, while evenness measures how similar species are in abundance [8]. Species richness and evenness are two independent diversity measure criteria that may differ in their response to local habitat factors [8]. Recent studies have shown that the relationship between richness and evenness appears weaker than expected [9]. These two diversity components may vary and could be influenced by different ecological factors. For instance, extreme weather in a highly diversified forest may cause species extinction, reducing species richness but increasing the distribution's evenness. Other studies have also demonstrated that species evenness could impact ecosystem productivity and other functions, as species richness does [10]. It is, therefore, logical that species evenness and richness are both considered to gain a deeper understanding of the effects of different species diversity patterns [11].

Various indices have been proposed to capture information about the species diversity of a plant community [12]. The main objective of a diversity index is to obtain a quantitative estimate of biological variability that can be used to compare biological entities in space or time. Species diversity indices can, therefore, be divided into simple and composite indices [13]. The most common simple index is species richness. However, this index usually under-emphasizes species abundance information [14]. Composite indices combine species richness and evenness into a single value and are widely used in ecology. These indices have the benefits of being simple to calculate and having a long application history. However, most of them prefer to express the information of only one component between richness and evenness and sacrifice the information of another component, such as the Shannon–Wiener ( $H'$ ) and Simpson index ( $D_2$ ), which are the most used indices for describing species diversity in forest ecosystems [15]. A major additional drawback of a composite index is the ambiguity in its definition [15]. For example, the Shannon–Werner index can be interpreted as a measure of the uncertainty in the identity of an individual randomly selected from a community, where a higher degree of uncertainty implies greater diversity. The Simpson index is a probability that does not have a straightforward, ecologically meaningful interpretation [16]. From this perspective, it is necessary to consider all four diversity indicators: species richness, species evenness, Shannon–Wiener index, and Simpson diversity index to compensate for the weaknesses in each diversity index. This will give a much more detailed understanding of the forest diversity, considering the richness, evenness, abundance, and relative abundance among the other indicators.

Species diversity can be defined as the variability of living organisms in an ecosystem [4]. It may also be considered the diversity between and within species in a particular ecosystem [17]. Species diversity is a significant ecosystem component due to its role in the hydrological cycle and climate regulation [18]. Species diversity has declined globally despite the enactment of global conservation agreements, such as the Convention on Biological Diversity (CBD), in which most biodiversity hotspots are found in the tropics [19]. For instance, after decades of forest destruction, the tropical forests in Ghana have experienced extensive species extinction and diversity loss. Of the more than 2100 plant species found in forest zones of Ghana, 23 are endemic. Seven hundred and thirty economic tree species in the forest zones, most of which have a dimension of 5 cm or more at breast height, are

threatened or extinct [20]. Hence, the effective conservation of tree diversity in the tropical forests of Ghana is a critical priority, requiring the establishment of an effective approach capable of identifying early warning signs of diversity change at multiple scales [21]. This information is crucial for designing and introducing policies and management actions to halt the decline in tree diversity and create more resilient forest areas [22].

Remote sensing technology plays a crucial role in supporting biodiversity monitoring. Remote sensing data can provide information on an area to various extents, with shorter revisit times and lower costs than classical field surveys. Huesca et al. [23] argued that traditional field surveys are mostly costly and involve a lot of time and financial resources with lower spatial extents. The Landsat satellite series has provided valuable data for monitoring and mapping the Earth's surface for over 40 years [2]. The Landsat-8 satellite, launched in 2013, enhanced the imaging capacity of this series, introducing new spectral bands in the blue and short-wave infrared (SWIR) ranges and improving the sensor signal/noise ratio and the image radiometric resolution [3]. The Operational Land Imager (OLI) sensor supplies optical images with 30 m spatial resolution, eight spectral bands, and 16 days of temporal resolution [4]. Sentinel-2, a multispectral sensor of medium spatial resolution produced by the European Space Agency (ESA), was conceived to ensure the continuity of global data on the Earth's surface. This mission was launched in 2015 and presented a wide swath (290 km), a revisit time (five days, with two satellites), a medium spatial resolution (10, 20, and 60 m), and a relatively good number of spectral bands (13).

Landsat and Sentinel data have been used to assess tropical forest diversity. Madonsela et al. [2] identified the best vegetation index (NDVI, EVI, SAVI, and SRI) in estimating species diversity by comparing vegetation indices in Landsat 8 multispectral data with alpha-diversity index (Shannon index, species richness index, and Simpson index), using principal component analysis (PCA). Kumar et al. [4] calculated forest species diversity with information-theory-based indices using Sentinel-2 sensors. While medium-resolution data provide some spatial detail compatible with the size of vegetation units and biomass field observations, obtaining cloud-free, high spatial, temporal, and spectral resolution imagery is usually problematic. Hence, properly assessing tropical forest species diversity might not be feasible. Although there are usually trade-offs in the properties of satellite sensors, such as spatial resolutions and temporal revisit time, studies have shown that obtaining optimal spatial, spectral, and temporal information is vital for better forest structure estimation [21,24,25].

The recent advancement in CubeSat, a small satellite composed of a 1U unit ( $10 \times 10 \times 10 \text{ cm}^3$ ) with a mass of 1.33 kg [26], provides unique spatial and temporal observations due to large constellations of small satellites. PlanetScope, provided by Planet, comprises one of the largest CubeSat constellations. With more than 130 satellites, the PlanetScope satellites enable daily observations with approximately 3.7 m spatial resolution. Although spectral resolution and radiometric consistency should be considered, the frequent observation and high spatial resolution of the PlanetScope data offer new opportunities for land cover monitoring. Several studies have used PlanetScope data for forest cover and structural mapping [27–30].

The retrieval of biophysical variables based on remote sensing data is derived from a preferred individual spectral wavelength range, such as the red-edge band, which highlights vegetation vigor. Alternatively, a spectral index is employed as a proxy for a vegetation trait [31]; for instance, the NDVI is a popular and frequently used spectral index. According to Peng et al. [32], the most common and best vegetation index in estimating  $S$ ,  $H$  and  $D_2$  index is the EVI, NDVI, SAVI, and SRI because they can minimize atmospheric noise and soil background and improve the estimation of plant species diversity in a dense canopy.

Considering that the PlanetScope data allows almost daily images over an area with a spatial resolution of 3 m and eight spectral bands, and the fact that not enough research has made use of the PlanetScope data in assessing forest species diversity, this research explores the potential for using PlanetScope to assess and predict tropical species diversity.

This research is guided by the following research question: (1) What is the relationship between species diversity and the spectral bands of PlanetScope data? (2) How can species diversity be best predicted based on the PlanetScope data? The findings of this study will help inform biodiversity conservation and the management of BFRs.

## 2. Materials and Methods

### 2.1. Study Area

This study was conducted in the BFR in southern Ghana, in the Ashanti Region (Figure 1). The reserve lies between latitude  $6^{\circ} 40'$  and  $6^{\circ} 44'$  North of the Equator and longitudes  $1^{\circ} 15'$  and  $1^{\circ} 22'$  West of the Greenwich. It is approximately 25 km northeast of Kumasi, Ashanti's regional capital. The BFR covers an area of roughly 30 square kilometers. This forest is part of the tropical rainforest biome of West Africa, which exhibits high biodiversity, and it is home to various plant and animal species, including endemic and endangered species [33]. The forest structure is characterized by an upper canopy layer comprising a mixture of deciduous and evergreen species in approximately equal proportions. The average canopy height is approximately 40 m, with emergent trees up to 60 m tall. Common species found in this study area include *Celtis zenkeri*, *Celtis milbraedii*, *Triplochiton scleroxylon*, *Sterculia rhinopetala*, *Funtumia elastica*, *Baphia nitida*, *Cleidion gabonicum*, *Nesogordonia papaverifera*, *Hymnostegia afzeli*, *Turraenthus africanus*, and *Trichilia prieuriana* (Djagblatey) [34]. The landscape is undulating with a 6–7% slope and an elevation between 180 m and 245 m above sea level. The soil varies from sandy to clay and passes into gray-leached sandy or silty soil [34]. The study area experiences a tropical climate with distinct wet and dry seasons. The site has a bimodal rainfall regime known as the major and minor seasons, with the major typically starting from April to July, followed by the little dry season in August, and the minor season continues from September to November, followed by the main dry season in December, [35]. Annual rainfall in the forest varies between 1200 and 1750 mm. The mean yearly maximum temperature ranges between  $30.9$  and  $31.6$  °C, averaging  $31.1$  °C.

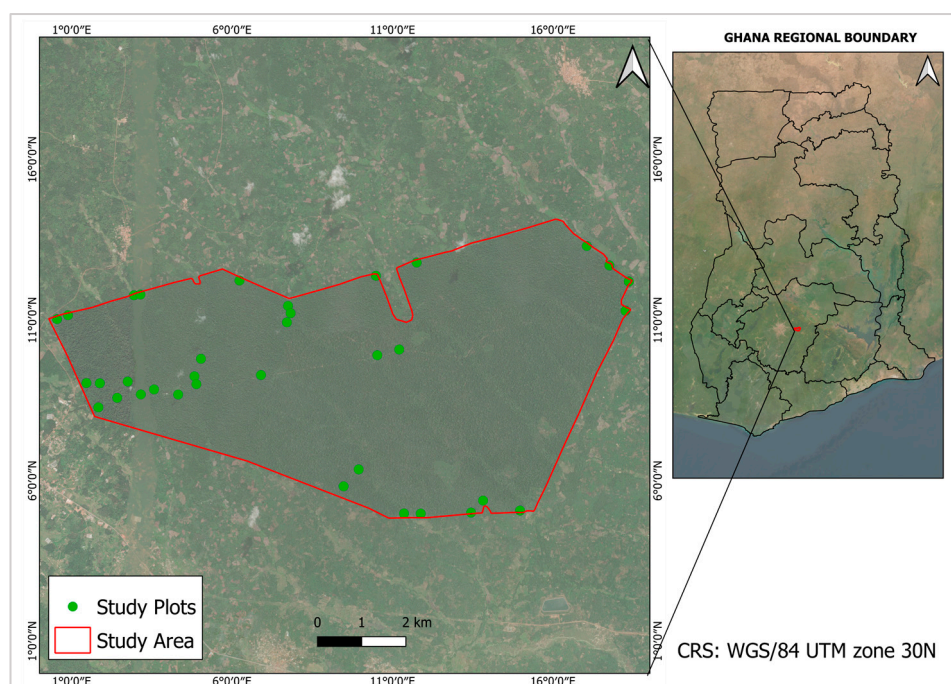


**Figure 1.** Study location (Bobiri Forest Reserve, Ghana).

### 2.2. Remote Sensing Data Acquisition and Preprocessing

PlanetScope data with a 3 m spatial resolution from Planet Lab Inc. (Kurfürstendamm, Berlin, Germany) [36] was used in this study. All spectral bands were included (i.e.,

blue, green, green, yellow, red, red edge, and near-infrared (NIR); Table 1), except for the coastal blue band, with nearly daily global coverage. The PlanetScope data, available at <https://www.planet.com/> (accessed on 6 September 2023), was accessed through a research and education license.

**Table 1.** PlanetScope spectral band description.

Dataset	Spatial Resolution (m)	Band Name/Number	Wavelength (nm)	Date of Image Acquisition
PlanetScope	3.0	Blue	465–515	19 April 2023
		GreenI *	513–549	
		Green	547–585	
		Yellow *	600–620	
		Red	600–620	
		RedEdge *	697–713	
		NIR	845–885	

All spectral bands that were used for processing and extraction with their wavelengths and band names. \* Only included when ordering 8-band bundles.

We used the PlanetScope surface reflectance product, incorporating geometric, radiometric, and atmospheric corrections [36]. To retain as much good data as possible, the acquisition date was set to the closest period of the data collection, May 2023, that met the following criteria: “standard” quality level, no cloud cover, and images that fell within a subset area. We used the surface reflectance scenes because the surface reflectance data preserves calculated pixel values, no color balancing or adjustments are applied, and with adequate preprocessing, they are suitable for use cases such as forest and crop health monitoring and wildfire assessment, among others [37]. Consequently, four scenes of already mosaiced images for the targeted subset devoid of cloud cover were downloaded. The next step was to perform a subset of the image using an ROI (region of interest) (Figure 2). Furthermore, we used the pixel extraction tool in SNAP with a window size of  $3 \times 3$ , which is the closest to the plot size. We selected mean as the aggregation method to extract the spectral reflectance values of each band within the PlanetScope image for all plots.

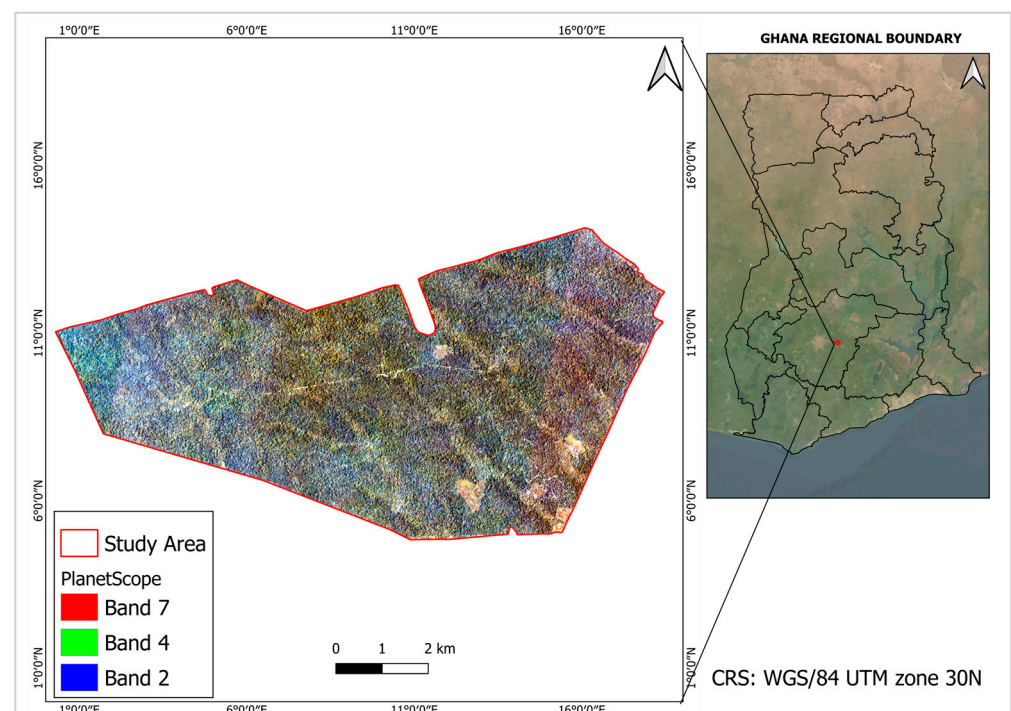


**Figure 2.** Preprocessed RGB composite of PlanetScope data.

Finally, the forward stepwise regression method was used to check the influence of potential predictors, in this case, the spectral reflectance bands and VIs, on the outcome of the two main species diversity indices ( $S$  and  $H'$ ). At each step, variables were chosen based on their Akaike's information criterion (AIC), which was used to limit the total number of variables included in the final model. According to Pearse et al. [38], the stepwise selection of variables is a useful and effective data analysis tool when the outcome being studied is relatively new, the importance of individual covariates may not be known, and associations with the outcome are not well known, which is the case in this research.

### 2.3. Tree Species Data

#### 2.3.1. Field Sampling Protocol and Tree Species Data Collection

Mapfumo et al. [39] and Mutowo et al. [40] have proven that sampling of plot sizes widely used ranges between 20 and 200 m<sup>2</sup> in tall shrub communities and 200–25,000 m<sup>2</sup> for tall trees in woods and forests. Their research guided us in selecting the plot size for species sampling. Tree species were sampled from 35 plots with a 20 m × 50 m plot size. A simple random sampling approach was used to define the placement of the plots following the research conducted by Oli et al. [41], with a minimum distance of 200 m apart to avoid overlapping of sampling plots [42]. Although this was the original protocol, we sampled the plots according to the accessible areas because of the inaccessibility of some parts of the forest. A mobile device with a field map application and Global Positioning System functionality was used to record plot coordinates. Three hundred and eleven individual tree species of the 15 most dominant within the forest were sampled, and their diameter at breast height (DBH) ≥ 5 cm was recorded using a diameter tape. The maximum heights of the trees were recorded using a TruePulse device. Species identification was performed with the help of a plant taxonomist, and the nomenclature was verified using the readily available online repository The World Flora Online [43]. The 15 most dominant tree species in the study area were identified. This was determined through engagement with individuals who worked within the Forest Reserve and the staff at the Forestry Research Institute of Ghana (FORIG). The collection of tree species data was conducted in June 2023.

#### 2.3.2. Estimating the Diversity of Tree Species

The  $H'$  and  $D_2$  are the most frequently used indices in ecological literature, according to Mandosola et al. [44] and Peng et al. [32]. Tree species diversity was quantified in each plot using four diversity measures.  $S$ ,  $J'$ ,  $H'$ , and  $D_2$  (Table 2). Although  $H'$  and  $D_2$  consider both species richness (the number of different species) and abundance (the number of individual trees within species), these aspects of diversity have a bearing on the spectral signal captured by the remote sensing device [45]; hence, they were computed separately to test their relationship with the spectral reflectance of the bands and vegetation indices.

**Table 2.** Vegetation indices used in this study and their equations.

Vegetation Index	Equation	Reference
Normalized difference vegetation index (NDVI)	$NDVI = \frac{NIR - RED}{NIR + RED}$	[46]
Enhanced vegetation index (EVI)	$EVI = G \times (NIR - RED) / (NIR + C1 \times RED - C2 \times BLUE + L)$	[47]
Simple ratio index (SRI)	$SRI = \frac{NIR}{RED}$	[48]
Soil-adjusted vegetation index (SAVI)	$SAVI = \frac{NIR - RED}{(NIR + RED + L)} \times (1 + L)$	[49]
Normalized difference red edge index	$NDRE = \frac{NIR - RE_{EDGE}}{(NIR + RE_{EDGE})}$	[50]

$L$  is a soil fudge factor that varies from 0 to 1 depending on the soil coefficients adopted in the MODIS-EVI algorithm are  $L = 1$ ,  $C1 = 6$ ,  $C2 = 7.5$ , and  $G = 2.6$ .

#### 2.4. Relationship between Tree Species Diversity Indices and Remotely Sensed Data

Using stepwise linear regression analysis, we investigated the relationships between species diversity indices (Table 3) with response variables and spectral band information (Table 1) as predictor variables. The root mean square error (RMSE), coefficient of determination ( $r^2$ ), and Akaike's information criterion (AIC) of the regression guided the selection of the most appropriate model to show species diversity. The prediction model had the smallest RMSE and AIC, and the highest  $r^2$ . According to Peng et al. [32], the RMSE measures how close the model predicts field measurements,  $r^2$  measures the proportion of variance in the dependent variable predicted from the independent variable, and AIC estimates the quality of each model relative to the other models. In addition to the regression, we evaluated the correlation between variables using Pearson's correlation coefficients.

**Table 3.** Diversity indices used in this study and their equations.

Species Diversity Index	Equation	Reference
Species richness	$S = N$	[12]
Simpson index	$D_2 = 1 / \sum_{i=1}^S p_i^2$	[12,51]
Shannon index	$H' = - \sum_{i=1}^S p_i \ln(p_i)$	[12,52]
Species evenness	$J' = - \sum_{i=1}^S p_i \ln(p_i) / \ln(S)$	[53]

where  $N$  is the total number of tree species in a sample;  $p_i$ , the proportional abundance of species  $I$  relative to the total abundance of all species  $S$  in a plot  $\ln(p_i)$  is the natural logarithm of this proportion.

### 3. Results

The predominant species (top six) identified in the BFR were *Sterculia rhinopetala*, *Triplochiton scleroxylon*, *Celtis milbraedae*, *Cola gigantia*, and *Hymenostegia afzelii* (Table 4). Among the tree species selected for this study, the highest number of individual trees was recorded for *Sterculia oblonga*. In contrast, the lowest number of individual trees was recorded for *Baphia pubescens*.

**Table 4.** Tree species list and their frequencies within the study area.

Family	Scientific Names	Number of Individual Tree Species
1. Leguminosae-Papilionoideae	<i>Baphia pubescens</i>	16
2. Leguminosae-Caesalpinioideae	<i>Bussea occidentalis</i>	18
3. Ulmaceae	<i>Celtis zenkeri</i>	19
	<i>Celtis mildbraedii</i>	27
4. Malvaceae	<i>Cola caricifolia</i>	17
	<i>Cola giganti</i>	26
	<i>Nesogordonia papaverifera</i>	18
	<i>Pterygota macrocarpa</i>	20
	<i>Sterculia Oblonga</i>	20
5. Meliaceae	<i>Sterculia rhinopetala</i>	28
	<i>Triplochiton scleroxylon</i>	27
	<i>Carapa Procera</i>	18
6. Apocynaceae	<i>Funtumia elastica</i>	18
7. Simaroubaceae	<i>Hannoa klaineana</i>	14
8. Leguminosae	<i>Hymenostegia afzelii</i>	25
Total		311

#### 3.1. Correlation between Diversity Indices and Remotely Sensed Data

Using a Pearson correlation matrix, we performed a correlation analysis between the diversity indices, spectral bands, and vegetation indices.  $S$  and  $H'$  are the diversity variables that correlated significantly with the spectral bands and VIs.  $D_2$  and  $J'$  showed no significant correlation with the spectral bands and VIs. Regarding the spectral bands,

our results showed bands 6, 5, 4, 3, and 2 (red, yellow, green, greeni, and blue) correlated with  $S$  and  $H'$ ; however, band 6 had the highest correlation with  $S$ , with a correlation coefficient of 0.61 and  $p < 0.001$ . Similarly, spectral bands 6, 5, 4, 3, and 2 demonstrated a positive correlation with  $H'$ ; however, band 6 showed the highest correlation with  $H'$ , with a coefficient of 0.58 and  $p < 0.01$ . Almost all VIs (NDVI, NDRE, SAVI, SRI) demonstrated a negative correlation with both  $S$  and  $H'$ ; however, NDRE showed the highest correlation with a coefficient of  $-0.48$  and  $p < 0.05$ , followed by the NDVI with a correlation coefficient of 0.17 for  $S$  and 0.40 for  $H$ , and  $p < 0.5$  for both  $S$  and  $H'$  (Figure 3).

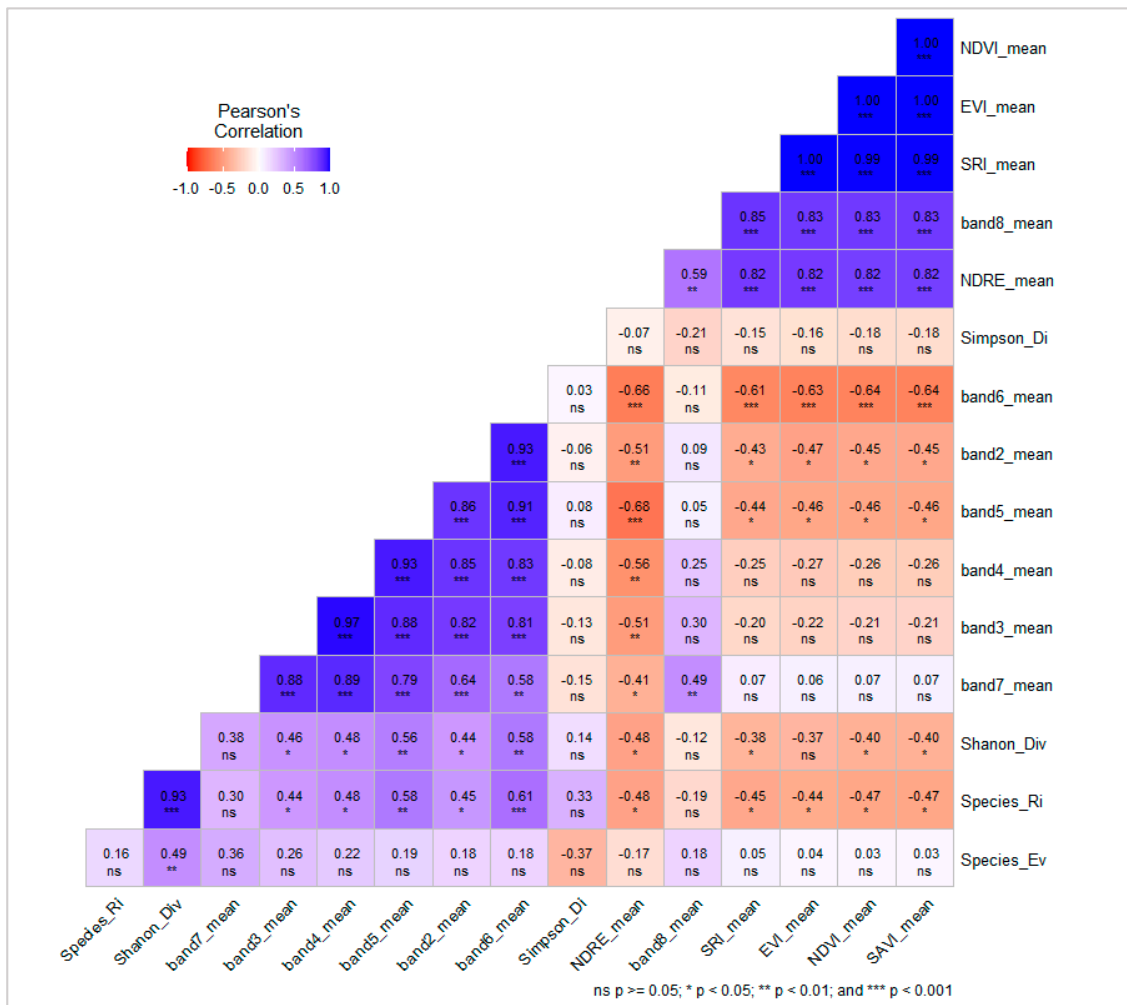


**Figure 3.** Correlation matrix between diversity indices, spectral bands, and vegetation indices: band2\_mean = mean of spectral band 2, band3\_mean = mean of spectral band 3, band4\_mean = mean of spectral band 4, band5\_mean = mean of spectral band 5, band6\_mean = mean of spectral band 6, band7\_mean = mean of spectral band 7, band8\_mean = mean of spectral band 8, NDVI\_mean = mean of the NDVI, EVI\_mean = mean of the EVI, SAVI\_mean = mean of the SAVI, SRI\_mean = mean of the SRI, NDRE\_mean = mean of the NDRE, Species\_Ri = species richness ( $S$ ), Species\_Ev = species evenness ( $J'$ ), Shanon\_Div = Shannon diversity index ( $H'$ ), and Simpson\_Di = Simpson diversity index ( $D_2$ ).

To predict species diversity within the BFR, a forward stepwise regression model with species richness and Shannon index as predictor variables and the mean spectral bands and VIs of the PlanetScope data as response variables were used to obtain the subset of variables that results in the best model. For species richness prediction, the stepwise model showed that mean spectral band 6 (red) and mean spectral band 2 (blue) were the most important variables that produced a good model with an ( $r^2 = 0.47$ ), (RMSE = 1.00) and (AIC = 85.15).

Similarly, for the prediction of the Shannon diversity index, mean spectral bands 6 and 2 produced a good model with an ( $r^2 = 0.42$ ), (RMSE = 0.17), and (AIC =  $-10.74$ ). We did not predict the Simpson diversity index and species evenness because they did not demonstrate a correlation with the spectral bands and VIs. The results show that the best models for estimating tree species diversity ( $S$  and  $H'$ ) using PlanetScope data were derived from spectral bands 6 and 2. The obtained model equations (Table 5) were used to calculate species richness and the Shannon diversity index in a GIS environment using the raster calculator function in QGIS. Figure 4 shows species diversity predicted maps ( $S$  and  $H'$ ) for the BFR. The diversity map (Figure 4a) shows species richness ( $S$ ) within the BFR. Some areas within the BFR had species richness between 2 and 4, while only smaller areas towards the south-east have a species richness of 5, with the rest showing species richness of 1. In general, species richness was fairly distributed across the study area. Also, the diversity map (Figure 4b) indicates that the Shannon diversity index within the BFR is generally moderately scattered over the entire region. Therefore, the results show some species diversity levels in the BFR.

**Table 5.** Regression equations for plant diversity prediction based on the best-predicted model with the lowest AIC and RMSE and the highest  $R^2$ .

Diversity Index	Regression Equation	$R^2$	RMSE	AIC
$S$	Species_Ri $\sim -4.23 + 23.45 \times \text{band6\_mean} - 22.18 \times \text{band2\_mean}$	0.47	1.00	85.15
$H'$	Shanon_Div $\sim 0.08 + 3.45 \times \text{band6\_mean} - 3.14 \times \text{band2\_mean}$	0.42	0.17	$-10.74$

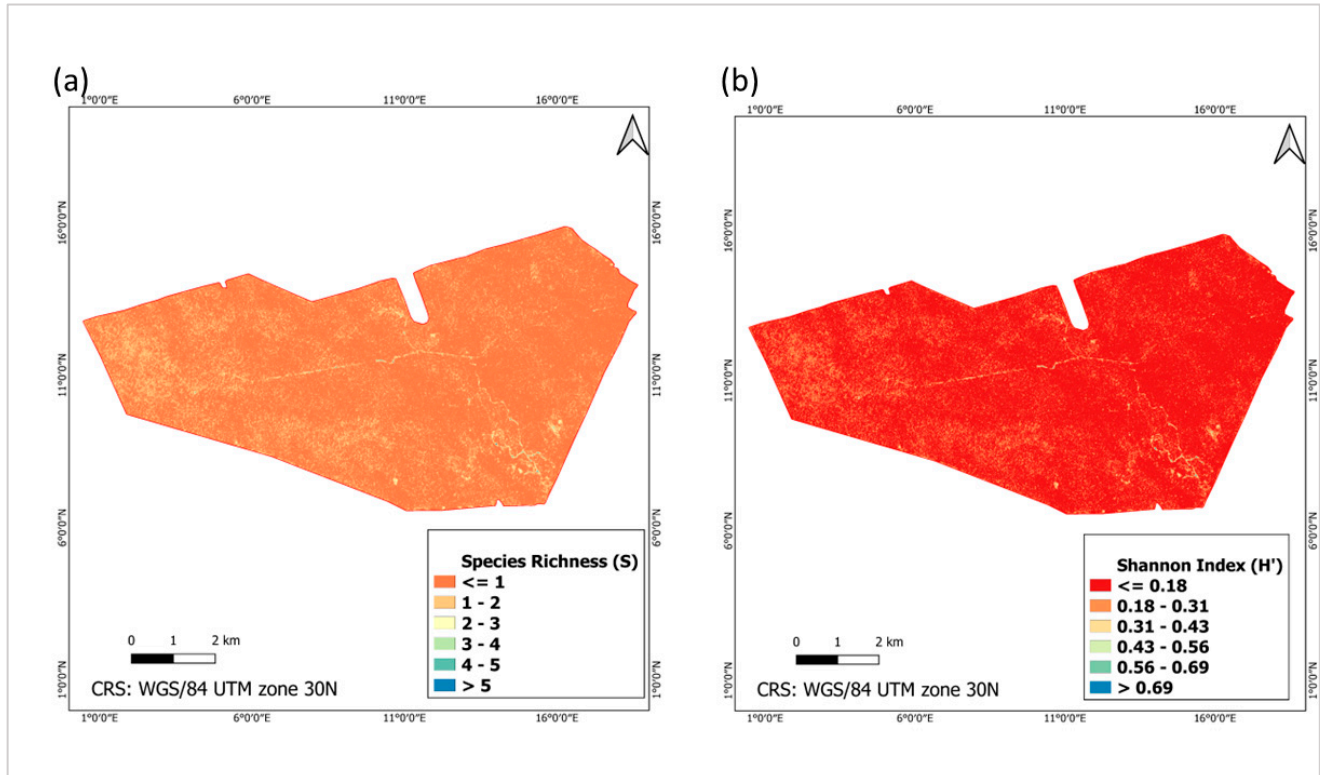


**Figure 4.** Species diversity thematic maps derived from the stepwise predicted model. (a)  $S$ —species richness (b)  $H'$ —Shannon index.

### 3.2. Stepwise Linear Regression for Species Diversity Prediction

The equations (Table 5) were employed to estimate  $S$  and  $H'$  by substituting the corresponding bands in the raster calculator in QGIS. The equations were used to predict  $S$  and  $H'$  across the study area. The resulting maps provide spatial insights into the distribution of predicted diversity values based on the spectral band information. The intercept ( $-4.23$ ) represents the estimated  $S$  when both the mean spectral of bands 6 and 2 are zero. The coefficient for the spectral mean of band 6 (23.45) indicates the estimated change in  $S$  for a one-unit increase in the mean of spectral band 6. The coefficient for the mean of spectral band 2 ( $-22.18$ ) indicates the estimated change in  $S$  for a one-unit increase in the mean of spectral band 2. For the  $H'$  prediction, the intercept (0.08) represents the estimated  $H'$  when both the spectral mean of bands 6 and 2 are zero. The coefficient of the spectral mean of band 6 (3.45) indicates the estimated change in  $H'$  for a one-unit increase in the spectral mean of band 6. The coefficient for the mean of spectral band 2 ( $-3.14$ ) indicates the estimated change in  $H'$  for a one-unit increase in the spectral mean of band 2. The positive coefficient for band 6 in both  $S$  and  $H'$  predictions suggests that higher values of this band are associated with increased  $S$  and  $H'$  while the negative coefficients for band 2 suggests that higher values of band 2 are associated with decreased  $S$  and  $H'$  (Table 5). For  $S$  prediction, the model achieved an  $R^2$  value of 1.00, indicating a good fit to the data, while for the prediction of  $H'$ , the model achieved an  $R^2$  value of 0.42 indicating that approximately 42% of the variability in the  $H'$  is explained by the model.

The models emphasize the importance of both bands in predicting species diversity, with specific bands 6 and 2 having different impacts on  $S$  and  $H'$ . The high  $R^2$  value for  $S$  may indicate a strong relationship between the selected bands and  $S$ , while the  $R^2$  value for  $H'$  suggests a moderate level of explanatory power.

## 4. Discussion

The BFR is one of Ghana's most important protected areas, incorporating local communities for biodiversity conservation [35]. The reserve has a wide range of indigenous tree species, approximately 120 bird species, and a butterfly sanctuary with about 340 butterfly species that can potentially contribute to economic growth through tourism [54]. Therefore, monitoring and assessing tree species diversity in the area is essential for sustainable conservation. Thus, understanding tree species diversity in biodiversity conservation is crucial because it provides reserve management with the necessary baseline information regarding the distribution of tree species and their changes within the forest reserve, which is essential in the planning and managing forest reserves. Remote sensing data provides valuable information to achieve such desired results.

The PlanetScope imagery is increasingly used for scientific applications focused on terrestrial ecosystems. A common use case is land cover and land use changes, where the spatial resolution and temporal frequency of the image can provide information related to fine-scale land cover changes that may not be captured by moderate resolution sensors such as Landsat 8 OLI and Sentinel-2 MSI [55,56]. Similarly, using PlanetScope imagery to estimate land surface phenology is a natural use case becoming more common. For example, John et al. [57] used PlanetScope imagery to detect the timing of flowering in alpine wildflowers in Washington State, Chen et al. [58] used PlanetScope imagery in combination with Sentinel-2 to monitor flowering phenology in almond orchards in the Central Valley of California. These studies have consistently demonstrated that PlanetScope imagery provides an effective basis for monitoring phenology from remote sensing. However, each of the studies discussed focuses on individual phenological events within ecosystems, and none has assessed the capabilities or potential of PlanetScope data in predicting species diversity. Our results demonstrate a significant relationship between some spectral bands of PlanetScope imagery and species diversity and the ability to predict species diversity with this spectral information.

The significant relationship between the spectral bands of PlanetScope data (red and blue) and species diversity variables ( $S$  and  $H'$ ) suggests that satellite images such

as PlanetScope would help predict biodiversity in tropical forests [3]. According to Badourdine [59], the green and red edge bands are particularly sensitive to photosynthetic pigment content, suggesting their link or relationship between taxonomic information, photosynthetic activity, and spectral information. Tesfaye and Awoke [60] also confirmed in their studies that the red band, which falls within the visible part of the electromagnetic spectrum, influences vegetation properties, such as canopy biomass and leaf chlorophyll content. Also, the red and blue bands are reported to be the chlorophyll absorption regions. Conti et al. [61] found that the blue band, which relates to pigments, including carotene and xanthophylls, tends to correlate with species diversity after performing a principal component analysis of all spectral bands with species diversity. With the area being a tropical, moist, semi-deciduous forest, and the study period rainy, vegetation in the area is assumed to have contained the chlorophyll pigments, carotene, and xanthophylls, culminating in the absorption of such chemicals and, thus, correlation with species diversity. Therefore, it is unsurprising that the red and blue bands had a significant relationship with tree species diversity, as measured by  $S$  and  $H'$  within the BFR.

Our findings are consistent with those of Gyamfi-Ampadu [62] and Imran et al. [63] who demonstrated that the red part of the spectrum, that is, the red band, was best for estimating species diversity, hence their correlation with the species diversity ( $S$  and  $H'$ ). It must also be noted that the reserve lies in Ghana's tropical moist, semi-deciduous south-east forest zone and hence receives higher annual rainfall and a short dry season. This situation ensures that the reserve is dominated by healthy vegetation. Although our results showed a correlation between species diversity and the red and blue bands, this correlation was positive, similar to Conti et al. [61]. The positive correlation between the diversity indices ( $S$  and  $H'$ ) and spectral reflectance of bands 6 and 2 of the PlanetScope data confirms their sensitivity to the nature and structure of the forest and the vegetation properties (Gyamfi-Ampadu) [62]. According to Kulawardhana [64], the positive correlation of spectral bands with species diversity is due to species-specific differences in pigment content, leaf structure, and canopy structural components such as leaf area index. Therefore, the importance of the visible bands in plant diversity prediction can be justified by the fact that this portion of the spectrum, especially bands in the red and blue, is the major leaf pigment absorption range, which is sensitive to mainly chlorophyll  $a$ , and  $b$  contents, according to the sensitivity analysis reported by Zhao et al. [65].

According to Cabacinha et al. [66], even though some authors like Foody and Cutler [67] have not found any strong correlations between vegetation indices and species diversity, one can expect a relationship between them since it is related to the richness, i.e., the number of species in the community, and the abundance representing the distribution of individuals by species. In the Pearson correlation performed to assess the relationship between  $H'$ ,  $S$ , and VIs,  $H'$  and  $S$  showed a better correlation with the NDVI ( $-0.47$ ), SAVI ( $-0.47$ ), and NDRE ( $-0.48$ ). This may be because the VIs were calculated using the NIR and red edge bands, which have been suggested for discriminating species diversity [32,68]. Additionally, according to Fajji et al. [69], different VIs are computed by combining two or more spectral bands, assuming that multi-band analysis would provide further information. Furthermore, the results of the study could be attributed to the sensitivity of the VIs to variability in vegetation characteristics, i.e., shape and size of the tree, water content, and associated background. The results could also be attributed to environmental factors such as the amount of rainfall and temperature received in the study area.

This finding is consistent with those of Arekhi et al. [68], who found the NDVI having the highest significant correlation with  $H'$  calculated from basal area ( $3 \times 3$  Shannon index basal area (SIBA) with  $r = 0.685$  in the Gonen Dam watershed in Turkey. Furthermore, the research of Gaitan et al. [70] showed a strong correlation between the NDVI and species richness in steppe ecosystems. According to Madonsela et al. [44], the differences in sensitivity to vegetation characteristics could be explained by the different measurement scales of the VIs. For instance, in the study of Rampheri et al. [71], the VIs that had a better relationship with  $H'$  (NDVI and SAVI) have a measurement scale that ranges from  $-1$  to

1. Overall, the type of forest and complexity of forest stands in terms of multi-layers and species composition can affect the outcome of estimations.

Similar to the correlation results, the stepwise regression analysis demonstrated that bands 2 (blue) and 6 (red) were the most important variables explaining species diversity. According to Rejauar et al. [72], the green and red bands are the two main absorption bands of two primary leaf pigments: The chlorophyll pigment (green pigments) and the Xanthophylls. These strong absorption bands induce a peak in the reflectance of the yellow–green bands (550 nm), so chlorophyll is called the green pigment. This accounts for the relationship observed in our results between the blue, green, and red bands with species diversity indices ( $S$  and  $H'$ ), which aligns with Mockel et al. [73].

The results of this study demonstrated variations in species diversity ( $S$  and  $H'$ ). The relatively high  $S$  within the study area can be attributed to the protected nature of the forest, with fewer human-induced activities and favorable conditions, such as humid and warm temperatures. For example, Li et al. [74] observed a high diversity of Salicaceae species in warm and wet areas other than regions in China. The increased rainfall in the area can also account for the relatively high species richness. Shoko et al. [75] found that environments with high soil moisture favor the increased production of C3 above-ground biomass (AGB). In addition, solar radiation in the area may cause a high evapotranspiration rate. According to these studies, solar radiation is the primary energy source that regulates terrestrial ecosystems' chemical, physical, and biological processes. Therefore, the evapotranspiration rate defines the species diversity [74,76]. Our results show moderate  $H'$  values, with some areas showing high values. In the research of Naidu et al. [77], they reported a Shannon–Wiener index ( $H'$ ) for all six plots varying from 3.59 to 4.05, which falls within the range of 0.67 to 4.86 reported in tropical forests in the Indian sub-continent [78]. These values correspond to the values obtained in our results.

Considering the results of this study, the use of remote sensing data (PlanetScope) to predict tree species diversity plays a vital role in conservation management. These results imply that PlanetScope spectral bands explain species diversity variations better than VIs. This demonstrates how ecological knowledge and satellite-based information can be effectively combined to address a wide range of current natural resource conservation/management challenges strategies.

## 5. Conclusions

This study provides insight into the usefulness of the spectral bands of PlanetScope data in predicting species diversity in a tropical forest such as the BFR. A correlation test assessed the relationship between spectral bands, VIs, and species diversities ( $S$  and  $H'$ ). Stepwise regression was also used to select the most important variable from all response variables, providing a good model for predicting species diversity. The results showed that the red and blue bands of the visible spectrum range are most important in predicting species diversity.

In conclusion, the BFR in Ghana is a vital protected area with a rich biodiversity, including numerous indigenous tree species and diverse bird and butterfly populations. The sustainable conservation of tree species diversity within this reserve is paramount as it provides baseline information for effective forest management. Even though the results show a prediction of species diversity, we recommend incorporating data from other sensors, such as lidar and radar, and environmental variables to improve such predictions.

**Author Contributions:** Conceptualization—E.N. and P.S. Methodology—E.N., J.N.O., R.T.G., B.E.A., R.K.N. and P.S. Investigation—E.N., J.N.O. and P.S. Original draft preparation—E.N. and J.N.O. Funding acquisition—E.N. and P.S. All authors have read and agreed to the published version of the manuscript.

**Funding:** This research was funded by the Faculty of Forestry and Wood Sciences—FFWS, Czech University of Life Sciences Prague, (IGA/FLD/A\_11\_23 (Internal grant number: 43140/1312/3189).

**Data Availability Statement:** Data are available upon request.

**Acknowledgments:** Many thanks to all the individuals and institutions that assisted with data collection of this study. Special acknowledgement the contributions of the Forestry and Research Institute of Ghana in Kumasi for their effective collaboration and willingness to provide all the needed assistance for the data collection campaign. Special thanks to the Staff of the Bobiri Forest Reserve (Manfred and Bolt) for their support and further assistance in acquiring data throughout the field campaign. We would like to specially acknowledge John Akomatey and Ebenezer Ampofo Nti (taxonomists) for their instrumental roles, assisting in the tree species identification.

**Conflicts of Interest:** The authors declare no conflict of interest. The funders had no role in the design of the study, in the collection, analyses, or interpretation of data, in the writing of the manuscript, or in the decision to publish the results.

## References

- Gamfeldt, L.; Snäll, T.; Bagchi, R.; Jonsson, M.; Gustafsson, L.; Kjellander, P.; Ruiz-Jaen, M.C.; Fröberg, M.; Stendahl, J.; Philipson, C.D.; et al. Higher levels of multiple ecosystem services are found in forests with more tree species. *Nat. Commun.* **2013**, *4*, 1340. [[CrossRef](#)] [[PubMed](#)]
- Qi, W.; Saarela, S.; Armston, J.; Ståhl, G.; Dubayah, R. Remote Sensing of Environment Forest biomass estimation over three distinct forest types using TanDEM-X InSAR data and simulated GEDI lidar data. *Remote Sens. Environ.* **2019**, *232*, 111283. [[CrossRef](#)]
- Madonsela, S.; Azong, M.; Ramoelo, A.; Mutanga, O. Remote sensing of species diversity using Landsat 8 spectral variables. *ISPRS J. Photogramm. Remote Sens.* **2017**, *133*, 116–127. [[CrossRef](#)]
- Kumar, P.; Dobriyal, M.; Kale, A.; Pandey, A.K.; Tomar, R.S.; Thounaojam, E. Calculating forest species diversity with information-theory based indices using sentinel-2A sensor's of Mahavir Swami Wildlife Sanctuary. *PLoS ONE* **2022**, *17*, e0268018. [[CrossRef](#)] [[PubMed](#)]
- Tindan, P.D. Savanna primary livelihoods at the edge of land degradation: Linkages and impacts in Ghana. *Int. J. Innov. Appl. Stud.* **2015**, *10*, 119–131.
- Behera, S.R.; Dash, D.P. The effect of urbanization, energy consumption, and foreign direct investment on the carbon dioxide emission in the SSEA (South and Southeast Asian) region. *Renew. Sustain. Energy Rev.* **2017**, *70*, 96–106. [[CrossRef](#)]
- Vaglio Laurin, G.; Puletti, N.; Hawthorne, W.; Liesenberg, V.; Corona, P.; Papale, D.; Chen, Q.; Valentini, R. Discrimination of tropical forest types, dominant species, and mapping of functional guilds by hyperspectral and simulated multispectral Sentinel-2 data. *Remote Sens. Environ.* **2016**, *176*, 163–176. [[CrossRef](#)]
- Buckland, S.T.; Magurran, A.E.; Green, R.E.; Fewster, R.M. Monitoring change in biodiversity through composite indices. *Philos. Trans. R. Soc. B Biol. Sci.* **2005**, *360*, 243–254. [[CrossRef](#)]
- Soininen, J.; Passy, S.; Hillebrand, H. The relationship between species richness and evenness: A meta-analysis of studies across aquatic ecosystems. *Oecologia* **2012**, *169*, 803–809. [[CrossRef](#)]
- Zhang, Y.; Chen, H.Y.H.; Reich, P.B. Forest productivity increases with evenness, species richness and trait variation: A global meta-analysis. *J. Ecol.* **2012**, *100*, 742–749. [[CrossRef](#)]
- Crowder, D.W.; Northfield, T.D.; Gomulkiewicz, R.; Snyder, W.E. Conserving and promoting evenness: Organic farming and fire-based wildland management as case studies. *Ecology* **2012**, *93*, 2001–2007. [[CrossRef](#)]
- Morris, E.K.; Caruso, T.; Buscot, F.; Fischer, M.; Hancock, C.; Maier, T.S.; Meiners, T.; Müller, C.; Obermaier, E.; Prati, D.; et al. Choosing and using diversity indices: Insights for ecological applications from the German Biodiversity Exploratories. *Ecol. Evol.* **2014**, *4*, 3514–3524. [[CrossRef](#)] [[PubMed](#)]
- Chao, A.; Wang, Y.T.; Jost, L. Entropy and the species accumulation curve: A novel entropy estimator via discovery rates of new species. *Methods Ecol. Evol.* **2013**, *4*, 1091–1100. [[CrossRef](#)]
- Wilsey, B.J.; Chalcraft, D.R.; Bowles, C.M.; Willig, M.R. Relationships among indices suggest that richness is an incomplete surrogate for grassland biodiversity. *Ecology* **2005**, *86*, 1178–1184. [[CrossRef](#)]
- Hakkenberg, C.R.; Song, C.; Peet, R.K.; White, P.S. Forest structure as a predictor of tree species diversity in the North Carolina Piedmont. *J. Veg. Sci.* **2016**, *27*, 1151–1163. [[CrossRef](#)]
- Tuomisto, H. A consistent terminology for quantifying species diversity? Yes, it does exist. *Oecologia* **2010**, *164*, 853–860. [[CrossRef](#)] [[PubMed](#)]
- Pimentel, D.; Stachow, U.; Takacs, D.A.; Brubaker, H.W.; Amy, R.; Meaney, J.J.; Neil, J.A.S.O.; Onsi, D.E.; Corzilius, D.B.; Dumas, A.R.; et al. Conserving Biological Diversity in Most biological diversity exists in Agricultural/Forestry Systems. *Bioscience* **1992**, *42*, 354–362. [[CrossRef](#)]
- Hector, A.; Bagchi, R. Biodiversity and ecosystem multifunctionality. *Nature* **2007**, *448*, 188–190. [[CrossRef](#)]
- Myers, N.; Mittermeier, R.A.; Mittermeier, C.G.; da Fonseca, G.A.B.; Kent, J. Biodiversity hotspots for conservation priorities. *Nature* **2000**, *403*, 853–858. [[CrossRef](#)]
- Appiah, M. Tree population inventory, diversity and degradation analysis of a tropical dry deciduous forest in Afram Plains, Ghana. *For. Ecol. Manag.* **2013**, *295*, 145–154. [[CrossRef](#)]

21. Chrysafis, I.; Korakis, G.; Kyriazopoulos, A.P.; Mallinis, G. Predicting tree species diversity using geodiversity and sentinel-2 multi-seasonal spectral information. *Sustainability* **2020**, *12*, 9250. [[CrossRef](#)]
22. Nagendra, H.; Lucas, R.; Honrado, J.P.; Jongman, R.H.G.; Tarantino, C.; Adamo, M.; Mairota, P. Remote sensing for conservation monitoring: Assessing protected areas, habitat extent, habitat condition, species diversity, and threats. *Ecol. Indic.* **2013**, *33*, 45–59. [[CrossRef](#)]
23. Huesca, M.; Merino-de-miguel, S.; Eklundh, L.; Litago, J.; Cicuéndez, V.; Rodríguez-rastrero, M.; Ustin, S.L.; Palacios-orueta, A. Ecosystem functional assessment based on the “optical type” concept and self-similarity patterns: An application using MODIS-NDVI time series autocorrelation. *Int. J. Appl. Earth Obs. Geoinf.* **2015**, *43*, 132–148. [[CrossRef](#)]
24. Astola, H.; Häme, T.; Sirro, L.; Molinier, M.; Kilpi, J. Comparison of Sentinel-2 and Landsat 8 imagery for forest variable prediction in boreal region. *Remote Sens. Environ.* **2019**, *223*, 257–273. [[CrossRef](#)]
25. Fagua, J.C.; Jantz, P.; Rodríguez-buritica, S.; Duncanson, L.; Goetz, S.J. Integrating LiDAR, Multispectral and SAR Data to Estimate and Map Canopy Height in Tropical Forests. *Remote Sens.* **2019**, *11*, 2697. [[CrossRef](#)]
26. Mura, M.; Botalico, F.; Giannetti, F.; Bertani, R.; Mancini, M.; Orlandini, S.; Travaglini, D.; Chirici, G. Exploiting the capabilities of the Sentinel-2 multi spectral instrument for predicting growing stock volume in forest ecosystems. *Int. J. Appl. Earth Obs. Geoinf.* **2018**, *66*, 126–134. [[CrossRef](#)]
27. Riihimäki, H.; Luoto, M.; Heiskanen, J. Remote Sensing of Environment Estimating fractional cover of tundra vegetation at multiple scales using unmanned aerial systems and optical satellite data. *Remote Sens. Environ.* **2019**, *224*, 119–132. [[CrossRef](#)]
28. Csillik, O.; Kumar, P.; Mascaro, J.; Shea, T.O.; Asner, G.P. Monitoring tropical forest carbon stocks and emissions using Planet satellite data. *Sci. Rep.* **2019**, *9*, 17831. [[CrossRef](#)] [[PubMed](#)]
29. Baloloy, A.B.; Blanco, A.C.; Candido, C.G.; Argamosa, R.J.L.; Dumlalag, J.B.L.C.; Dimapilis, L.L.C.; Paringit, E.C. Estimation of mangrove forest aboveground biomass using multispectral bands, vegetation indices and biophysical variables derived from optical satellite imageries: Rapideye, planetscope and sentinel-2. *ISPRS Ann. Photogramm. Remote Sens. Spat. Inf. Sci.* **2018**, *4*, 29–36. [[CrossRef](#)]
30. Mulatu, K.A.; Decuyper, M.; Brede, B.; Kooistra, L.; Reiche, J.; Mora, B.; Herold, M. Linking Terrestrial LiDAR Scanner and Conventional Forest Structure Measurements with Multi-Modal Satellite Data. *Forests* **2019**, *10*, 291. [[CrossRef](#)]
31. Viña, A.; Gitelson, A.A.; Nguy-robotson, A.L.; Peng, Y. Remote Sensing of Environment Comparison of different vegetation indices for the remote assessment of green leaf area index of crops. *Remote Sens. Environ.* **2011**, *115*, 3468–3478. [[CrossRef](#)]
32. Peng, Y.; Fan, M.; Song, J.; Cui, T.; Li, R. Assessment of plant species diversity based on hyperspectral indices at a fine scale. *Sci. Rep.* **2018**, *8*, 4776. [[CrossRef](#)] [[PubMed](#)]
33. Baffour-Ata, F.; Antwi-Agyei, P.; Nkiaka, E. Climate variability, land cover changes and livelihoods of communities on the fringes of bobiri forest reserve, Ghana. *Forests* **2021**, *12*, 278. [[CrossRef](#)]
34. Djagbletey, G. Impact of Selective Logging on Plant Diversity, Natural Recovery and Vegetation Carbon Stock: The Case of Bobiri Forest Reserve. Ph.D. Thesis, Kwame Nkrumah University of Science and Technology, Kumasi, Ghana, 2014.
35. Addo-Fordjour, P.; Anning, A.K.; Larbi, J.A.; Akyeampong, S. Liana species richness, abundance and relationship with trees in the Bobiri forest reserve, Ghana: Impact of management systems. *For. Ecol. Manag.* **2009**, *257*, 1822–1828. [[CrossRef](#)]
36. Planet Labs. Planet Imagery Product Specifications. Web Document. 2019. Available online: <https://assets.planet.com/docs/combined-imagery-product-spec-april-2019.pdf> (accessed on 6 September 2023).
37. Wang, J.; Yang, D.; Detto, M.; Nelson, B.W.; Chen, M.; Guan, K.; Wu, S.; Yan, Z.; Wu, J. Multi-scale integration of satellite remote sensing improves characterization of dry-season green-up in an Amazon tropical evergreen forest. *Remote Sens. Environ.* **2020**, *246*, 111865. [[CrossRef](#)]
38. Pearce, J.; Ferrier, S. An evaluation of alternative algorithms for fitting species distribution models using logistic regression. *Ecol. Model.* **2000**, *128*, 127–147. [[CrossRef](#)]
39. Mapfumo, R.B.; Murwira, A.; Masocha, M.; Andriani, R. The relationship between satellite-derived indices and species diversity across African savanna ecosystems. *Int. J. Appl. Earth Obs. Geoinf.* **2016**, *52*, 306–317. [[CrossRef](#)]
40. Mutowo, G.; Murwira, A. Relationship between remotely sensed variables and tree species diversity in savanna woodlands of Southern Africa. *Int. J. Remote Sens.* **2012**, *33*, 6378–6402. [[CrossRef](#)]
41. Oli, B.N.; Subedi, M.R. Effects of management activities on vegetation diversity, dispersion pattern and stand structure of community-managed forest (*Shorea robusta*) in Nepal. *Int. J. Biodivers. Sci. Ecosyst. Serv. Manag.* **2015**, *11*, 96–105. [[CrossRef](#)]
42. Paudel, S.; Sah, J.P. Effects of Different Management Practices on Stand Composition and Species Diversity in Subtropical Forests in Nepal: Implications of Community Participation in Biodiversity Conservation. *J. Sustain. For.* **2015**, *34*, 738–760. [[CrossRef](#)]
43. WFO. Wold Flora Online. Published on the Internet. 2021. Available online: <https://about.worldfloraonline.org>. (accessed on 6 September 2023).
44. Madonsela, S.; Cho, M.A.; Ramoelo, A.; Mutanga, O.; Naidoo, L. Estimating tree species diversity in the savannah using NDVI and woody canopy cover. *Int. J. Appl. Earth Obs. Geoinf.* **2018**, *66*, 106–115. [[CrossRef](#)]
45. Oldeland, J.; Wesuls, D.; Rocchini, D.; Schmidt, M.; Jürgens, N. Does using species abundance data improve estimates of species diversity from remotely sensed spectral heterogeneity? *Ecol. Indic.* **2010**, *10*, 390–396. [[CrossRef](#)]
46. Rouse, R.W.H.; Haas, J.A.W.; Deering, D.W. *Monitoring Vegetation Systems in the Great Plains with ERTS*; NASA Special Publication: College Station, TX, USA, 1974.
47. Huete, A.R. A soil-adjusted vegetation index (SAVI). *Remote Sens. Environ.* **1988**, *25*, 295–309. [[CrossRef](#)]

48. Tucker, C.J. Red and Photographic Infrared Linear Combinations for Monitoring Vegetation. *Remote Sens. Environ.* **1979**, *8*, 127–150. [[CrossRef](#)]
49. Huete, A.; Justice, C.; Van Leeuwen, W. Modis Vegetation Index (mod 13). In *Algorithm Theoretical Basis Document Version 3*; NASA: Washington, DC, USA, 1999; pp. 295–309.
50. Modzelewska, A.; Stereńczak, K.; Mierczyk, M.; Maciuk, S.; Bałazy, R.; Zawila-Niedzwiecki, T. Sensitivity of vegetation indices in relation to parameters of Norway spruce stands. *Folia For. Pol. Ser. A* **2017**, *59*, 85–98. [[CrossRef](#)]
51. Simpson, E. Measurement of Diversity. *Nature* **1949**, *163*, 688. [[CrossRef](#)]
52. Shannon, C. A Mathematical Theory of Communication By c. E. Shannon Introduction. *Bell Syst. Tech. J.* **1948**, *27*, 519–520. [[CrossRef](#)]
53. Carlo, H.R.; Herman, P.; Soetaery, K. Indices of diversity and evenness. *Oceanis* **1998**, *24*, 61–87.
54. Mensah, I.; Ernest, A. Community Participation in Ecotourism: The Case of Bobiri Forest Reserve and Butterfly Sanctuary in Ashanti Region of Ghana. *Am. J. Tour. Manag.* **2013**, *2013*, 34–42.
55. Loranty, M.M.; Davydov, S.P.; Kropp, H.; Alexander, H.D.; Mack, M.C.; Natali, S.M.; Zimov, N.S. Vegetation Indices Do Not Capture Forest Cover Variation in Upland Siberian Larch Forests. *Remote Sens.* **2018**, *10*, 1686. [[CrossRef](#)]
56. Pickering, J.; Tyukavina, A.; Khan, A.; Potapov, P.; Adusei, B.; Hansen, M.C. Using Multi-Resolution Satellite Data to Quantify Land Dynamics: Applications of PlanetScope Imagery for Cropland and Tree-Cover Loss Area Estimation. *Remote Sens.* **2021**, *4*, 2191. [[CrossRef](#)]
57. John, A.; Ong, J.; Theobald, E.J.; Olden, J.D.; Tan, A.; Hillerislambers, J. Detecting Montane Flowering Phenology with CubeSat Imagery. *Remote Sens.* **2020**, *12*, 2894. [[CrossRef](#)]
58. Cheng, Y.; Vrieling, A.; Fava, F.; Meroni, M.; Marshall, M.; Gachoki, S. Remote Sensing of Environment Phenology of short vegetation cycles in a Kenyan rangeland from PlanetScope and Sentinel-2. *Remote Sens. Environ.* **2020**, *248*, 112004. [[CrossRef](#)]
59. Badourdine, C. Exploring the link between spectral variance and upper canopy taxonomic diversity in a tropical forest: Influence of spectral processing and feature selection. *Remote Sens. Ecol. Conserv.* **2022**, *9*, 235–250. [[CrossRef](#)]
60. Aklilu Tesfaye, A.; Gessesse Awoke, B. Evaluation of the saturation property of vegetation indices derived from sentinel-2 in mixed crop-forest ecosystem. *Spat. Inf. Res.* **2021**, *29*, 109–121. [[CrossRef](#)]
61. Conti, L.; Malavasi, M.; Galland, T.; Komárek, J.; Lagner, O.; Carmona, C.P.; de Bello, F.; Rocchini, D.; Šimová, P. The relationship between species and spectral diversity in grassland communities is mediated by their vertical complexity. *Appl. Veg. Sci.* **2021**, *24*, 1–8. [[CrossRef](#)]
62. Gyamfi-Ampadu, E.; Gebreslasie, M.; Mendoza-Ponce, A. Evaluating multi-sensors spectral and spatial resolutions for tree species diversity prediction. *Remote Sens.* **2021**, *13*, 1033. [[CrossRef](#)]
63. Imran, H.A.; Gianelle, D.; Scotton, M.; Rocchini, D.; Dalponte, M.; Macolino, S.; Sakowska, K.; Pornaro, C.; Vescovo, L. Potential and Limitations of Grasslands  $\alpha$ -Diversity Prediction Using Fine-Scale Hyperspectral Imagery. *Remote Sens.* **2021**, *13*, 2649. [[CrossRef](#)]
64. Kulawardhana, R.W. Remote sensing of vegetation: Principles, techniques and applications. By Hamlyn G. Jones and Robin a Vaughan. *J. Veg. Sci.* **2011**, *22*, 1151–1153. [[CrossRef](#)]
65. Zhao, F.; Guo, Y.; Huang, Y.; Reddy, K.N.; Lee, M.A.; Fletcher, R.S.; Thomson, S.J. Early detection of crop injury from herbicide glyphosate by leaf biochemical parameter inversion. *Int. J. Appl. Earth Obs. Geoinf.* **2014**, *31*, 78–85. [[CrossRef](#)]
66. Cabacinha, C.D. Relationships between floristic diversity and vegetation indices, forest structure and landscape metrics of fragments in Brazilian Cerrado. *For. Ecol. Manag.* **2009**, *257*, 2157–2165. [[CrossRef](#)]
67. Foody, G.M.; Cutler, M.E.; Mcmorrow, J.; Pelz, D.; Tangki, H.; Boyd, D.S.; Douglas, I.A.N. Mapping the biomass of Bornean tropical rain forest from remotely sensed data. *Glob. Ecol. Biogeogr.* **2001**, *10*, 379–387. [[CrossRef](#)]
68. Arekhi, M.; Yılmaz, O.Y.; Yılmaz, H.; Akyüz, Y.F. Can tree species diversity be assessed with Landsat data in a temperate forest? *Environ. Monit. Assess.* **2017**, *189*, 586. [[CrossRef](#)]
69. Fajji, N.G.; Palamuleni, L.G.; Mlambo, V. Evaluating derived vegetation indices and cover fraction to estimate rangeland aboveground biomass in semi-arid environments. *S. Afr. J. Geomat.* **2017**, *6*, 333–348. [[CrossRef](#)]
70. Gaitán, J.J.; Bran, D.; Oliva, G.; Ciari, G.; Nakamatsu, V.; Salomone, J.; Ferrante, D.; Buono, G.; Massara, V.; Humano, G.; et al. Evaluating the performance of multiple remote sensing indices to predict the spatial variability of ecosystem structure and functioning in Patagonian steppes. *Ecol. Indic.* **2013**, *34*, 181–191. [[CrossRef](#)]
71. Rampheri, M.; Dube, T.; Dhau, I. Use of remotely sensed data to estimate tree species diversity as an indicator of biodiversity in Blouberg Nature Reserve, South Africa. *Geocarto Int.* **2022**, *37*, 526–542. [[CrossRef](#)]
72. Rejaaur, R.; Hassan Abu, H.I. NDVI Derived Sugarcane Area Identification and Crop Condition Assessment. *Plan Plus* **2004**, *1*, 2.
73. Möckel, T.; Dalmayne, J.; Schmid, B.C.; Prentice, H.C.; Hall, K. Airborne hyperspectral data predict fine-scale plant species diversity in grazed dry grasslands. *Remote Sens.* **2016**, *8*, 133. [[CrossRef](#)]
74. Li, W.; Shi, M.; Huang, Y.; Chen, K.; Sun, H.; Chen, J. Climatic change can influence species diversity patterns and potential habitats of salicaceae plants in China. *Forests* **2019**, *10*, 220. [[CrossRef](#)]
75. Shoko, C.; Mutanga, O.; Dube, T. Remotely sensed C3 and C4 grass species aboveground biomass variability in response to seasonal climate and topography. *Afr. J. Ecol.* **2019**, *57*, 477–489. [[CrossRef](#)]
76. Silva, B.; Álava-Núñez, P.; Strobl, S.; Beck, E.; Bendix, J. Area-wide evapotranspiration monitoring at the crown level of a tropical mountain rain forest. *Remote Sens. Environ.* **2017**, *194*, 219–229. [[CrossRef](#)]

- 
77. Naidu, M.T.; Premavani, D.; Suthari, S.; Venkaiah, M. Assessment of tree diversity in tropical deciduous forests of Northcentral Eastern Ghats, India. *Geol. Ecol. Landsc.* **2018**, *2*, 216–227.
  78. Panda, P.C.; Mahapatra, A.K.; Acharya, P.K.; Debata, A.K. Plant diversity in tropical deciduous forests of Eastern Ghats, India: A landscape level assessment. *Int. J. Biodivers. Conserv.* **2013**, *5*, 625–639.

**Disclaimer/Publisher’s Note:** The statements, opinions and data contained in all publications are solely those of the individual author(s) and contributor(s) and not of MDPI and/or the editor(s). MDPI and/or the editor(s) disclaim responsibility for any injury to people or property resulting from any ideas, methods, instructions or products referred to in the content.